

Refereed Proceedings

*The 13th International Conference on
Fluidization - New Paradigm in Fluidization
Engineering*

Engineering Conferences International

Year 2010

EXPERIMENTAL QUANTIFICATION
OF THE SOLIDS FLUX IN AN
INTERNALLY CIRCULATING
FLUIDIZED BED

Trevor D. Hadley*

Christian Doblin, José Orellana†

Kok-Seng Lim‡

*IRO Process Science and Engineering, Australia, trevor.hadley@csiro.au

†CSIRO Process Science and Engineering, Australia

‡CSIRO Process Science and Engineering, Australia

This paper is posted at ECI Digital Archives.

http://dc.engconfintl.org/fluidization_xiii/117

EXPERIMENTAL QUANTIFICATION OF THE SOLIDS FLUX IN AN INTERNALLY CIRCULATING FLUIDIZED BED

Trevor D. Hadley, Christian Doblin, José Orellana, Kok-Seng Lim
CSIRO Process Science and Engineering
Bayview Avenue, Clayton, VIC 3168, Australia

ABSTRACT

Internally circulating fluidized beds (ICFBs) have been applied to a number of processes and provide a means of exchanging the bed particles from one reaction chamber to the other. Fundamental to this system is a good knowledge of the solids circulation rate (SRR). This paper summarises experimental investigations conducted using a hot tracer technique to measure the solids recirculation flux through an ICFB with a reaction and heat exchange chamber. Possible predictive models which link the bed hydrodynamics to the SRR are also evaluated.

INTRODUCTION

Solid particle circulation systems are commonly used when there are two or more connected reaction chambers which require a continuous movement of solids between the chambers. In fluidized bed processing these can be categorised as being externally circulating or internally circulating systems. The externally circulating systems are usually characterised by a solids riser (first chamber) connected to a cyclone and then a transfer of the solids to the second chamber via a downcomer and loopseal. The internally circulating fluidized bed (ICFB) system is an alternative design which has been applied to a number of processes such as coal/ biomass combustion and gasification, solid waste incineration as well as continuous adsorption and desorption (1). In such systems, the fluidization vessel is divided into compartments or chambers which are connected to each other. The recirculation of solids can be achieved by optimising the differential superficial gas velocity between the separate fluidized bed chambers. The chambers can take the form of a draft tube within an annulus (1,2) or be separated by using vertical plates (baffles) (3,4), vertical walls fitted with orifices (5) or even a combination of these (6).

By separating the fluidized bed into various chambers one is able to impose different reaction regimes, such as oxidising and reducing environments. One is also able to fluidize each chamber using a different gas as well as in different fluidization regimes. Another arrangement is to separate the reaction chamber from a heat recovery chamber (3,4). In this case, the solid particles pass through the fluidized bed reaction chamber and are then circulated into a separate fluidized bed heat exchange chamber where they are cooled or heated in order to regulate the bed temperature. This is the arrangement which has been considered in this study.

In order to design and operate an ICFB successfully, a good knowledge of the solids recirculation rate (SRR) is required. The SRR dictates the solids residence time in each chamber and hence the extent of reaction and heat transfer. Experimentally, the SRR can be determined from the vertical flux of material through one or more of the chambers using a range of methods such as multi-fibre optical probes (7), radiotracer particles (8), and hot tracer techniques (1,2).

Experimental data on the SRR in a fluidized bed reactor system with heat exchange tubes specific to our intended application is lacking. The paper therefore focuses on the experimental quantification of the extent of solids recirculation rate in such a reactor system using a hot particle tracer technique. Possible predictive models that relate the SRR to the bed hydrodynamic parameters are also evaluated and discussed in this paper.

EXPERIMENTAL SETUP

Fluidized Bed Reactor Model

SRR measurements were conducted in a fluidized bed reactor model (1.0 m x 0.5 m external plan dimensions) as shown in Figure 1a. The fluidized bed reactor has three, inter-connected fluidized bed chambers, with the central chamber representing the "reaction chamber" (RX), and a chamber on each side representing heat exchanger chambers (HEX). The chambers were separated by vertical baffles with slots in the lower section to enable the return of solids. The cross-sectional (XS) areas of the RX and HEX were (0.32 m x 0.46 m) and (0.30 m x 0.44 m) respectively. The baffle height, which influences the overall bed height, was designed at 0.4 m from the distributor. The heat exchanger tube bundle model was constructed of 25 mm diameter solid wooden dowels. A staggered tube arrangement with triangular pitch (2.5 times the diameter of the heat exchange tube based on centre-to-centre distance) was used. The HEX was also equipped with six sensitive platinum resistance temperature detectors (RTDs) with sensitivity of 0.01°C to assist SRR measurement. The RTDs were located at various positions within the tube bundle. In addition, pressure tapping points were installed at the bottom of the bed near the partitioning baffle as shown in Figure 1a.

Hot Solids Tracer / Injection System

Figure 1b shows the process flow diagram (PFD) of a hot-particle tracer injection system which was used to measure the SRR in the HEX. The hot tracer method has several advantages over other types of tracer techniques such as ease of application, no particle slip or segregation effects and avoidance of bed material contamination. In this approach, the tracer solids contained in a stainless steel vessel (up to 2 kg) were heated by an immersion heater (330 W) and an external band heater (200 W). An additional tape heater (150 W) was also used to heat the transfer line and minimise heat loss during solids injection into the bed. To achieve a faster heating rate, the particles in the heated vessel were also mildly fluidized by injecting air at the bottom of the vessel. The entire hot solids injection system was a self-contained unit including the vessel, support frames, vents, pneumatic actuated valves, electrical heating system and temperature controller.

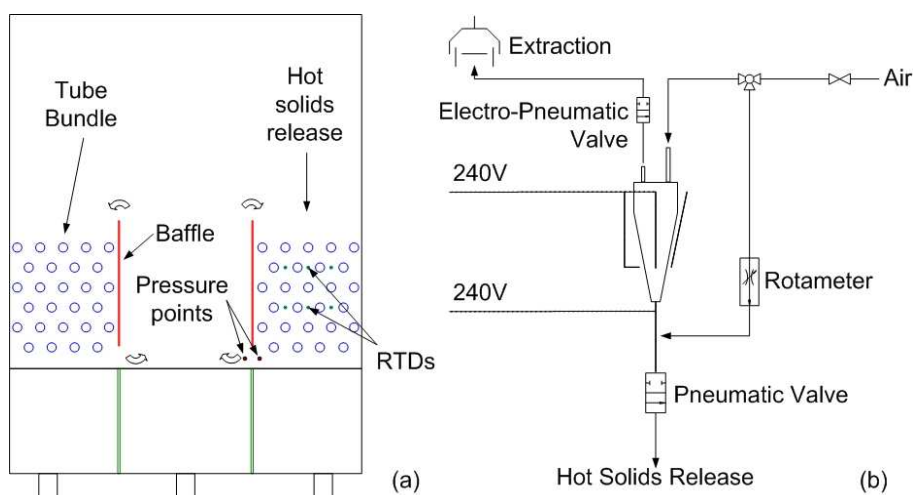


Figure 1. (a) Schematic diagram of the cold flow model, (b) PFD of the hot solids tracer/injection.

METHOD

The superficial fluidizing velocity in the central RX is generally set higher than that in the HEX. The differential velocity between the two chambers provides the necessary “driving force” (or pressure differential) to enable net recirculation of the solids from the HEX to the RX chamber.

The superficial fluidizing velocity in each chamber was controlled and monitored independently using either rotameters or orifice plates. In general, the superficial fluidizing velocity in the central RX (U_f) (0.12 – 0.50 m/s) was designed to be a multiple of the superficial fluidizing velocity in the HEX (U_m) (0.025 – 0.10 m/s), giving ratios (i.e. U_f/U_m) of around 2-7. In this study, the bed particles were glass ballotini with a mean particle size of 140 μm and particle density of 2600 kg/m^3 , giving an effective U_{mf} value of 15 mm/s based on the Wen and Yu correlation (9). As defined by the baffle’s vertical dimension, the bed height was maintained at 400 mm from the distributor.

Experiments were conducted to examine the influence of differential fluidizing velocity between the two inter-connected fluidized bed chambers on the net solids recirculation rate. In a typical solids flux experiment, the hot solids tracer (about 2 kg of bed material) was initially heated to 100°C in the holding vessel. The ICFB bed was then set at the pre-defined fluidization condition. At a predetermined time, the hot solids tracer material was discharged into the HEX just above the surface of the bed. The hot solids tracer was then dispersed and carried downwards by a net recirculation flow of solids through the HEX. The sensitive RTDs inserted into the HEX detected the temperature rise due to the arrival of hot solids as shown in Figure 2.

The vertical solids flux through the HEX was determined by analysing the time difference between peak temperatures between each vertical pair of RTDs, giving the effective time of travel of the bed solids within the HEX. As illustrated in Figure 2, the time difference between the two temperature peaks for RTDs No.2 and No.5 (i.e. 2-5 combination) was found to be 34.7 seconds. Since the distance between the two RTDs is known, the vertical solids velocity can be estimated. From this velocity, it

was possible to infer the solids recirculation flux by assuming a value of the bulk density as shown in Figure 2 (inset). Three measurements were repeated for each test condition to obtain the average value of the solids flux. Tests were carried out for a range of U_f and U_m conditions.

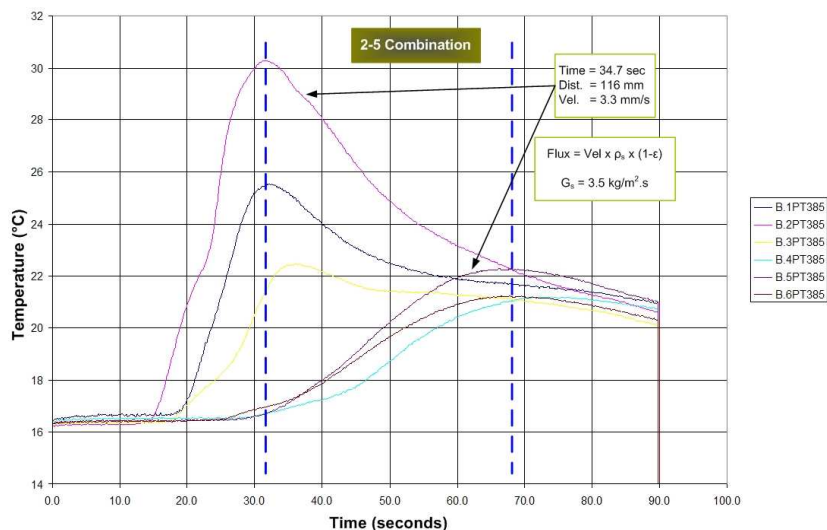


Figure 2. Typical transient temperature traces after injection of hot solids to determine SRR ($\rho_s = 2600 \text{ kg/m}^3$, $\epsilon = 0.6$).

RESULTS AND DISCUSSION

Figure 3 shows the measured SRR in the HEX as a function of the superficial fluidizing velocities, expressed in the form of $(U_f - U_{mf})/(U_m - U_{mf})$ - also referred as U_{Ratio} . The U_{Ratio} parameter was used as it was found to be more reflective of the bubbling flow phenomenon (i.e. excess gas flow) than the parameter based on U_f/U_m . The SRR values were found to increase with increasing U_{Ratio} . The differential gas velocity (ratio) clearly provides the dominant driving force to enable the net recirculation of solids between the two adjacent inter-connect chambers. In this instance, the solids fluxes were found to increase from 4 to 15 $\text{kg/m}^2.\text{s}$ within the range of U_{Ratio} from 2.5 to 6.5. Plotting the fluxes against the parameter U_{Ratio} , it was possible to clearly differentiate the influence of U_m on the SRR. Within the limits of the experimental variability, the measured SRRs were found to be greater in the bed with higher U_m . In general, the experimental results show similar trends to the findings of Jeon *et al* (1) where the vertical solids flux increased with an increase of superficial fluidizing velocity in the RX as well as the velocity in the HEX.

The results in this study, however, do not show indications of an asymptotic increase of the solids flux values at higher U_f values as found by Jeon *et al* (1). Unlike their study, the experiments presented here considered much lower U_f conditions which are below the limit of turbulent flow regime.

Theoretical Considerations

The SRR is influenced by a number of factors such as fluid and particle properties, gas velocity and bed geometry. The primary mechanism of net recirculation of solids is due to the bed hydrodynamic effect. To better optimise the performance of such

an inter-connected fluidized bed system, it is useful to examine the key driving forces that influence the solids recirculation behaviour.

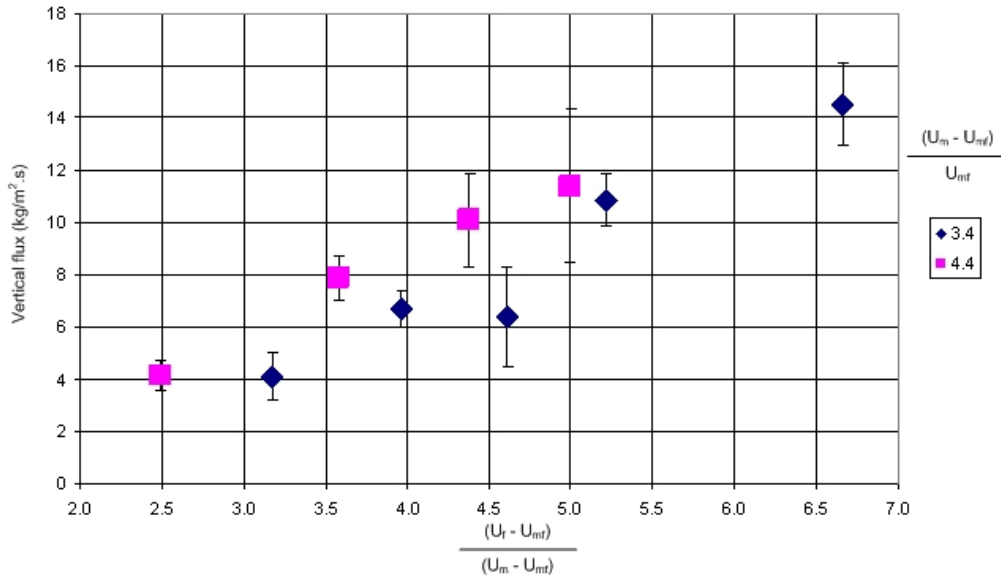


Figure 3. Plot of solids flux (based on free area in HEX) as a function of superficial fluidizing velocities.

As shown in Figure 4 (inset), the solid fluxes (movements) in the bed are due to the direct and indirect effects of bubble flow in the bed. The upward flow of the solids in the RX is due to the bubble drift and wake effects which can be described by (10):

$$G_{s,f} = f_w \epsilon_b U_b \rho_s (1 - \epsilon_{mf}) \quad [1a]$$

For high gas velocity, Equation [1a] can be simplified to the following expression:

$$G_{s,f} = f_w \rho_s (1 - \epsilon_{mf}) (U_f - U_{mf}) \quad [1b]$$

The solids flowing across the partitioning baffle (from the RX to the HEX), $G_{s,rt}$ is the result of bed expansion and bubble eruptions at the surface. As a result, $G_{s,rt}$ is defined to be a fraction of $G_{s,f}$ with a proportionality constant χ , i.e.:

$$G_{s,rt} = \chi G_{s,f} \quad [2]$$

The net downward flow of solids in the HEX is the difference of mass flow rates between the incoming $G_{s,rt}$ and outgoing $G_{s,o}$ solids fluxes. The $G_{s,o}$, representing the solids flux flowing through the underflow slot connecting the RX and HEX, is likened to the flow of a fluid through an opening (2,11) and can be estimated as follows:

$$G_{s,o} = C_D r \sqrt{2 \rho_s (1 - \epsilon) \Delta P / (1 - r^2)} \quad [3]$$

where r is the opening ratio, A_o / A_m and A_m is the available XS area in the HEX, not including the heat exchange tubes; and C_D is the effective discharge coefficient of the opening. The key driving force for the flow is the differential pressure across the orifice which can be approximated by the hydrostatic pressure difference, i.e.:

$$\Delta P = \Delta P_m - \Delta P_f = \rho_s g h (1 - \epsilon_{mf}) (\epsilon_{b,f} - \epsilon_{b,m}) \quad [4]$$

where ΔP_m and ΔP_f are the pressure drops across the bed in the RX and HEX respectively which can be approximated as follows:

$$\Delta P_m = (1 - \epsilon_{b,m}) (1 - \epsilon_{mf}) \rho_s g h \quad \Delta P_f = (1 - \epsilon_{b,f}) (1 - \epsilon_{mf}) \rho_s g h \quad [5a,b]$$

It can be seen that the effective differential pressure is due to the bubble voidage values (ϵ_b) in the two adjacent chambers. ΔP can be measured experimentally or

estimated by calculation based on bubble fraction determination. The key equations used in the determination of the bubble fraction are summarised in Table 1.

Table 1. Equations used in the determination of bubble fraction, hence bed pressure drop.

Parameter	Equation	Reference
Initial bubble size ¹	$d_{b0} = 2.78g^{-1}(U - U_{mf})^2$	(12)
Limiting bubble size (deep bed) ²	$d_{bm} = 1.633[(\pi/4)d_t^2(U - U_{mf})^{0.4}]$	(12)
Bubble diameter ^{2,3}	$d_b = d_{bm} - (d_{bm} - d_{b0})\exp(-0.3zd_t^{-1})$	(13)
Bubble rise velocity ⁴	$U_{br} = 0.711(gd_b)^{0.5}$	(14)
Bubble rise velocity ⁵	$U_{br} = 1.2[0.711(gd_b)^{0.5}]\exp(-1.49d_b d_t^{-1})$	(12)
Bubble velocity ^{2,3}	$U_b = 1.6\{(U - U_{mf}) + 1.13d_b^{0.5}\}d_t^{1.35} + U_{br}$	(15)
Bubble fraction ⁶	$\epsilon_b = (U - U_{mf}) / (U_b - U_{mf})$	(12)

1 for a perforated plate

2 for the HEX, d_t is determined based on the free area i.e. not including the heat exchange tubes

3 Geldart B powder

4 the rise velocity of a bubble with respect to the emulsion phase can be assumed to be the same as that of a single bubble (for $d_b/d_t < 0.125$ where wall effects are low) (12) [HEX]

5 the rise velocity of a bubble with respect to the emulsion phase when wall effects dominate [RX]

6 the bubbles in the HEX and RX are classified as being fast moving

For a specified operating mode under steady state conditions, the mass flow rates of solids (mass flow rate = $G_s A$) flowing through the different regions of the beds including across the orifice are equal and constant. The following section thus examines the relevance of the various parameters in relation to the estimation of the recirculation solids flux in such inter-connected fluidized beds.

Figure 4 shows the analysis results by comparing the experimentally measured solids fluxes in the HEX with different estimation methods (based on the free XS area in the HEX), namely equations [1, 2 and 3]. The upward solids fluxes estimated by equation [1], though similar in trend, are significantly greater than that measured experimental solids fluxes by an order of magnitude. However, a χ factor in the range of 5%, according to the method used in equation [2], could adequately match the experimental solids fluxes. This method also depicts the similar effect of gas velocity ratio including the influence of U_m , i.e. greater fluxes at higher U_m .

The pressure parameters used in equation [3] can be estimated from experiments or by using the bubble model calculation as suggested in Table 1. The solid fluxes estimated by equation [3], based on the experimentally measured pressures (at the base of the bed in each chamber), were also compared with the data. In this case, a C_D value of 0.2 was used, similar to that proposed by Song *et al* (2). The calculated results predicted values in a similar range but they showed low sensitivity to the superficial gas velocity ratio i.e. weaker influence. Whether the location of the pressure tapping played a role in the sensitivity of the pressure data was not determined. Alternatively, the solids fluxes were estimated by equation [3] but using the calculated pressure drop based on the approach suggested in Table 1. Using the same C_D value as suggested by Song *et al* (2), the calculated solids fluxes using this approach over-predicted the absolute values of experimental data although the trends are similar and show greater dependency on the velocity ratio when

compared with the previous approach using actual pressure measurements. The over prediction may be due to the bubble fraction estimation approach used in the HEX. There was no allowance made for the bubble fraction due to the presence of heat exchange tubes in the HEX. The bubble fraction in the HEX with tubes is generally expected to be higher according to Hull *et al* (16) due to close packing of the tubes, hence leading to a lower overall static pressure in the HEX. Consequently, the lower static pressure would give rise to a smaller differential pressure between the two separate chambers, hence lowering the effective solids fluxes according to the relationship expressed in equation [3].

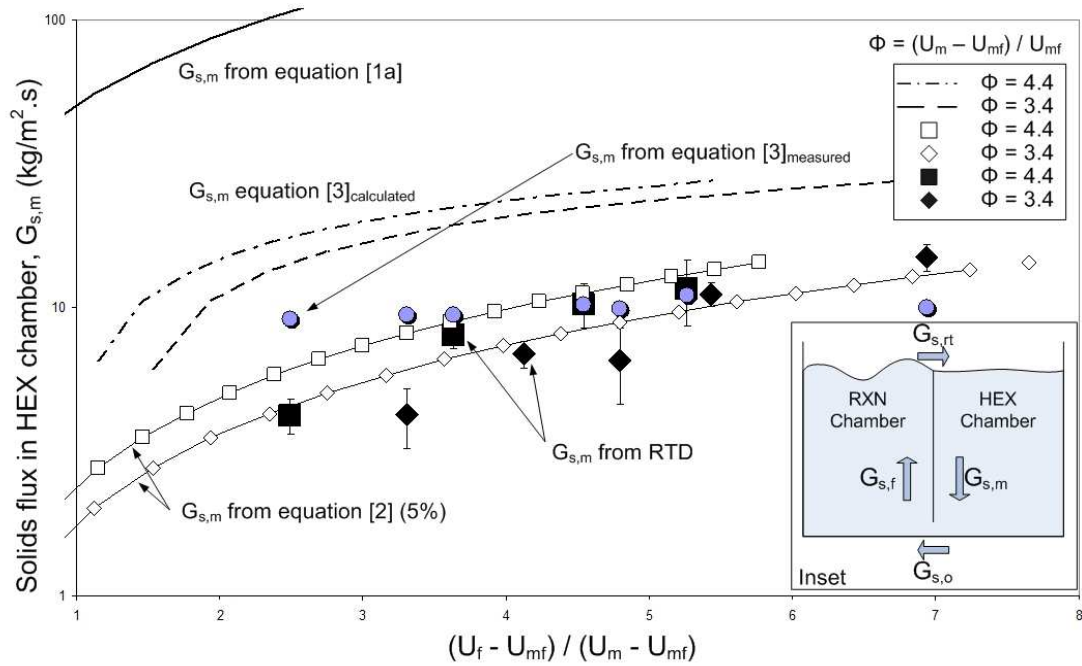


Figure 4. Comparison of calculated solids fluxes (based on HEX) with measured values.

In summary, the analysis above provided useful evaluation of the various approaches for the estimation of solids fluxes in the ICFB system. As expected, these models are limited at this stage to unequivocally predict the expected solids recirculation rate in a bed with heat exchange tubes and specific geometry. At this stage experimental measurement offers the only practical approach to quantify the solids recirculation, in the absence of more advanced models.

CONCLUSIONS

An experimental technique using hot solids tracer has been used effectively to quantify the solids recirculation rate (SRR) in an ICFB system with a heat exchange tube bundle. The SRR was found to be dependent on the gas velocity ratio between the two adjacent, interconnected fluidized bed chambers. The analysis shows that the available predictive models are still limited at this stage to unequivocally predict the expected solids recirculation rate in a bed especially with heat exchange tubes and specific bed geometry and design. Further model development is required.

NOTATION

A	cross-sectional area	m^2	f_w	wake fraction	-
d_b	effective bubble diameter	m	g	acceleration due to gravity	m/s^2
C_D	discharge coefficient	-	G_s	solids flux	$kg/m^2.s$
d_{bm}	maximum bubble diameter	m	h	height of the fluidized bed	m
d_{b0}	bubble diameter at the distributor	m	U	superficial fluidizing velocity	m/s
d_t	hydraulic diameter of the bed	m	z	distance above the distributor	m

Greek

ρ_s	particle density	kg/m^3	χ	factor	-
ε	bed voidage fraction	-	ε_b	bubble fraction	-

Subscripts

br	single bubble rising	mf	minimum fluidization
f	reaction chamber	o	opening below the baffle
m	heat exchange chamber	rt	over the top of the baffle

REFERENCES

1. J.H. Jeon, S.D. Kim, S.J. Kim, Y. Kang, Solid circulation and gas bypassing characteristics in a square internally circulating fluidized bed with draft tube, *Chemical Engineering and Processing: Process Intensification*, **47** 12 (2008) 2351-2360.
2. B.H. Song, Y.T. Kim, S.D. Kim, Circulation of solids and gas bypassing in an internally circulating fluidized bed with a draft tube, *Chemical Engineering Journal*, **68** 2-3 (1997) 115-122.
3. T. Ohshita, T. Higo, S. Kosugi, N. Inumaru, H. Kawaguchi, Internal Circulating Fluidized Bed Type Boiler and Method of Controlling the Same, Patent 5138982 (1992).
4. T. Ohshita, S. Nagato, N. Miyoshi, S. Toyoda, Pressurized Internal Circulating Fluidized-Bed Boiler, Patent 5313913 (1994).
5. M. Fang, C. Yu, Z. Shi, Q. Wang, Z. Luo, K. Cen, Experimental research on solid circulation in a twin fluidized bed system, *Chemical Engineering Journal*, **94** 3 (2003) 171-178.
6. F.F. Snieders, A.C. Hoffmann, D. Cheesman, J.G. Yates, M. Stein, J.P.K. Seville, The dynamics of large particles in a four-compartment interconnected fluidized bed, *Powder Technology*, **101** 3 (1999) 229-239.
7. M. Ishida, T. Shirai, A. Nishiwaki, Measurement of the Velocity and Direction of Flow of Solid Particles in a Fluidized-Bed, *Powder Technology*, **27** 1 (1980) 1-6.
8. R.D. Abellon, Z.I. Kolar, W. den Hollander, de Goeij, J. J. M., J.C. Schouten, van den Bleek, C. M., A single radiotracer particle method for the determination of solids circulation rate in interconnected fluidized beds, *Powder Technology*, **92** 1 (1997) 53-60.
9. C.Y. Wen, Y.H. Yu, A Generalized Method for Predicting Minimum Fluidization Velocity, *AIChE Journal*, **12** 3 (1966) 610-612.
10. D. Kunii, O. Levenspiel, Fluidization Engineering, Original Edition 1969 ed., John Wiley and Sons, New York, (1977).
11. D.R.M. Jones, J.F. Davidson, The flow of particles from a fluidised bed through an orifice, *Rheologica Acta*, **4** 3 (1965) 180-192.
12. D. Kunii, O. Levenspiel, Fluidization Engineering, Butterworth-Heinemann, Boston, (1991).
13. S. Mori, C.Y. Wen, Estimation of Bubble Diameter in Gaseous Fluidized-Beds, *AIChE Journal*, **21** 1 (1975) 109-115.
14. J.F. Davidson, D. Harrison, Fluidized Particles, Cambridge University Press, New York, (1963).
15. J. Werther, Hydrodynamics and mass transfer between the bubble and emulsion phases in fluidized beds for sand and cracking catalyst, In: Fluidization IV, (Ed. D. Kunii and R. Toei), Engineering Foundation, New York, (1984).
16. A.S. Hull, Z. Chen, J.W. Fritz, P.K. Agarwal, Influence of horizontal tube banks on the behavior of bubbling fluidized beds 1. Bubble hydrodynamics, *Powder Technology*, **103** 3 (1999) 230-242.

Keywords: Internally circulating fluidized bed, solids recirculation rate, solids flux prediction, hot tracer method, heat exchange system